Reactivity of Copper Electrodes towards Functional Groups and Small Molecules in the Context of CO_2 Electro-Reductions

Bernhard Schmid [1,2], Christian Reller [1], Sebastian S. Neubauer [1,3], Maximilian Fleischer [1], Romano Dorta [2] and Guenter Schmid [1,*

[1] Siemens AG, Corporate Technoloy, Research for Energy & Electronics, Guenther Scharowsky Strasse 1, 91058 Erlangen, Germany; schmid.bernhard@siemens.com (B.S.); christian.reller@siemens.com (C.R.); neubauer_sebastian@t-online.de (S.S.N.); maximilian.fleischer@siemens.com (M.F.)

[2] Lehrstuhl für Anorganische und Allgemeine Chemie, Friedrich Alexander Universität Erlangen-Nürnberg, Egerlandstraße 1, 91058 Erlangen, Germany; romano.dorta@fau.de

[3] Lehrstuhl für Physikalische Chemie I, Friedrich-Alexander-Universität Erlangen Nürnberg, Egerlandstraße 1, 91058 Erlangen, Germany

* Correspondence: guenter.schmid@siemens.com; Tel.: +49-913-173-2109

Abstract: The direct electro-reduction of CO_2 to functional molecules like ethene is a highly desirable variant of CO_2 utilization. The formation of, for example, ethene from CO_2 is a multistep electrochemical process going through various intermediates. As these intermediates are organic species, the CO_2 reducing electro-catalyst has to be competent for a variety of organic functional group transformations to yield the final product. In this work, the activity of an in situ-grown nano-structured copper catalyst towards a variety of organic functional group conversions was studied. The model reagents were selected from the product spectrum of actual CO_2 reduction reaction (CO_2RR) experiments and from proposals in the literature. The CO_2 bulk electrolysis benchmark was conducted at 170 mAcm^{-2} current density with up to 43% Faradaic Efficiency (FE) for ethene and 23% FE for ethanol simultaneously. To assure relevance for application-oriented conditions, the reactivity screening was conducted at elevated current densities and, thus, overpotentials. The found reactivity pattern was then also transferred to the CO reduction reaction (CORR) under benchmark conditions yielding additional insights. The results suggest that at high current density/high overpotential conditions, also other ethene formation pathways apart from acetaldehyde reduction such as CH_2 dimerization are present. A new suggestion for a high current density mechanism will be presented, which is in agreement with the experimental observations and the found activity pattern of copper cathodes toward organic functional group conversion.

Keywords: CO_2 electro-reduction; electro-catalytic mechanism; carbene carbonylation; electro-hydrogenation

1. Introduction

During the last few decades, researchers began tackling the problem of fossil fuel usage. The main task is the establishment of a closed carbon cycle and the implementation of renewable energy sources. Characteristic for the latter one are seasonal and weather-induced fluctuations [1,2]. To compensate for such intermittency, the installation of large overcapacities is necessary, which yet will produce stranded energy under optimal weather conditions. CO_2 electro-reduction is a feasible storage pathway for this stranded energy, which, at the same time, recycles emitted carbon, thus creating a closed carbon cycle [3,4]. These considerations have led to a vast increase of research efforts in CO_2 electro-reduction [5]. In this

context, copper seems to be a unique element that unifies the properties of a high H_2-overpotential enabling operation in low-cost aqueous electrolytes, comparably low CO_2-reduction overpotentials and being the only element featuring C–C–bond formation and formation of products originating from transfer of more than two electrons [6,7].

Products like ethene are of particular interest as their economic value as chemical feedstock exceeds their heating value by up to more than one order of magnitude (example in Supplementary Material (SM)). Pioneering work in CO_2 reduction was done by Hori [8] and Paik [9] on mercury electrodes. Copper-catalyzed CO_2 reduction to hydrocarbons was first reported by Hori in 1985 [10]. In the following decades, publications using copper electrodes [11–17], copper oxide electrodes [18–21], copper-containing perovskites [22], oxide-supported copper catalysts [23], halide-derived copper catalysts [24–27], copper-based alloys [28], copper-based metal-organic frameworks [29], molecular copper complexes [30], as well as alternative systems [5,31–36] vastly increased. Also pyridine-based co-catalysis known from Pd electrodes [37] could recently be transferred to copper-based systems [38]. Only recently, NiGa alloys have also been reported to produce trace amounts of ethene [39] and cobalt-proto-porphyrins producing methane [40].

Systematic catalyst development in this area requires a reliable model for the relationships between the products, intermediates and the catalyst properties. Understanding the mechanism is therefore a key to CO_2 electro-reduction as an applicable technology.

Attempts tackling the mechanism of CO_2 reduction by means of DFT-calculations [41–47], *in operando* spectroscopy [48–50] and surface science methods [21,50,51] are numerous. Yet, there is only one limited attempt of studying the reactivity of certain model compounds [52]. The research in this area is mainly focused on ethene, ethanol and formate and there is still lack of a general scheme covering all products. In this study, a more general approach to the mechanism was chosen. During the reduction of CO_2 to C2 or even C3 hydrocarbons and mono-oxygenates, the reaction goes through several electron transfer steps and numerous intermediates. These intermediates, however, have in common that they are organic or copper-organic species. The functional groups in these species are converted by electrochemical reduction into others in each step. Thus, studying the activity of a copper cathode catalyst towards reductive conversions of organic functional groups is a feasible way of tackling the mechanism. This method will elucidate which reactions are feasible to get from one intermediate to another, without limiting the understanding to a particular product. By this attempt, guidelines for mechanistic pathways can be obtained. Therefore, we conducted a screening at previously found optimum conditions by variation of 22 reactants.

It should be noted that the entire study was deliberately executed far from reaction onsets at potentials <-1 V vs. Reversible Hydrogen Electrode (RHE), as they occur at application relevant current densities. In contrast, the majority of mechanistic studies is conducted at close-to-onset potentials and therefore does not reach application relevant current densities. These conditions are often chosen to avoid non-equilibrium conditions and the corresponding local gradients, such as high pH values, concentration gradients and high overpotentials. In this study, these conditions are regarded as an inevitable aspect of applied CO_2RR and it is intended to reevaluate concepts found for close-to-onset conditions under high current density conditions.

2. Results and Discussion

2.1. CO2 Bulk Electrolysis Benchmark

We recently introduced a nano-scale copper dendrite electro-catalyst, which on a carbon gas diffusion layer (GDL) is capable of achieving over 50% Faradaic Efficiency (FE) for ethene at 170 mAcm^{-2} [53,54]. For this screening, this was the model catalyst of choice.

The catalyst is grown in situ from an acidic 6.4 mM $CuSO_4$ solution. The unique feature of this catalyst is its fine nano-scale dendrite structure, which creates many high index planes that are known

to be beneficial for ethanol evolution [55]. This structure is created by the templating effect of hydrogen bubbles, which are present due to the high current density and the low initial pH [56].

To be able to properly reflect the product scope of actual CO_2RR in the choice of the model reagents, the liquid phase products were also analyzed in the same 10 min time grid as the gaseous products. The FEs of all major gaseous and liquid products are compiled in Figure 1.
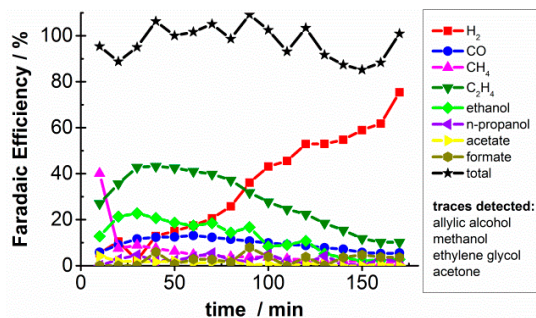
Figure 1. Faradaic Efficiency (FE) vs. time for major products of CO_2 bulk electrolysis at 170 mAcm^{-2}.

The main liquid phase product was ethanol. Besides, also *n*-propanol, acetate, ethylene glycol and formate (FE 2%–5%) and traces of allyl alcohol, methanol and acetone (FE < 1%), were quantified.

Noteworthy, the liquid analysis revealed an excellent performance of the catalyst also for ethanol formation in addition to the ethene performance. The FE for ethanol reached 23% after 30 min of electrolysis, which equals a partial current density of 39.1 mAcm^{-2}. This is among the highest reported values for ethanol. The Kenis group has reported an even higher value of 53 mAcm^{-2}, yet in an open system with a non-cycled KOH electrolyte at pH = 14 [57]. In our closed electrolyte cycle, which is closer to a continuously operable setup, using KBr and $KHCO_3$, the pH sets to ~7 due to the CO_2/HCO_3-buffer. Figure S35 (SM) gives evidence for this buffer along with working electrode (WE) potential and voltage data for the experiments.

In terms of functional groups, the products spectrum of CO_2RR features alkanes, electron-rich alkenes, carboxylates, terminal alcohols and ketones. The model reagents were chosen accordingly. On the other hand, the product scope lacks aldehydes, secondary alcohols, electron-deficient alkenes and alkynes. However, their absence may be explained either by lack of a formation pathway or by very high reactivity. Therefore, these classes are actually candidates for highly reactive intermediates. In addition, suggestions from the literature as glyoxal (20) or ethylene glycol (21) were also evaluated.

2.2. Model Reagent Screening

The screening was conducted on freshly prepared in situ-grown model catalyst on a solid copper support as also described in the previous work [54]. This method is more feasible for liquid or solid model reagents and allowed more precise measurements due to the reduced electrolyte volumes. The reagents are tested by addition of a sub-stoichometric amount (with respect to the total charge) after 10 min of catalyst deposition time. The galvanostatic bulk electrolysis strategy has the advantage that also reactions with lower onset potentials and with low Faradaic Efficiencies can be observed. Experiments with authentic products/intermediates are depicted in the suggested mechanism in Scheme 1. Additional model reactions are illustrated in Scheme 2.

Table S2 in the Supplementary Materials (SM) compiles important reactivity data obtained from each reactant. The given potentials are average values for the WE potential 50 s after addition of a reacting reactant. Those substrates usually cause a spontaneous distinctive rise of the potential, while it remains practically constant for inert or poorly reacting substrates. Examples of working electrode potential curves for both reacting and inert substrates are compiled in Figure S27 (SM). We also identified the subsiding of hydrogen evolution as a descriptive feature for the feasibility of a transformation. Also, CO_2RR itself is a competing process to the hydrogen evolution reaction

(HER). Thus, reactions that cannot compete with the HER are unlikely to participate in the mechanism. Notable changes in the electrolyte conductivity due to small volumes and the Nafion® separator lead to corruption of the IR-drop compensation. Table S2 (SM) therefore shows uncompensated values. Additional Spectra, GC data and exemplary electrical parameters are compiled in the Supplementary Materials (SM).
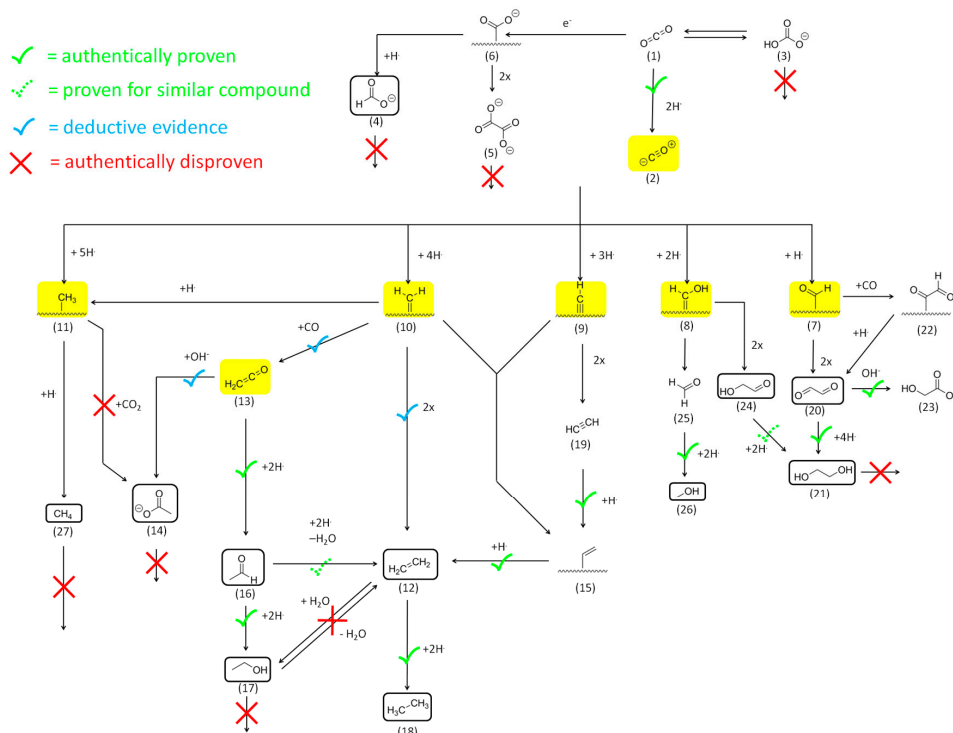
Scheme 1. Proposed mechanism for CO_2 electro-reduction on copper-based electrodes. Experimentally disproven pathways are indicated by a red cross. Detectable products are shown with a black frame, key intermediates are highlighted.
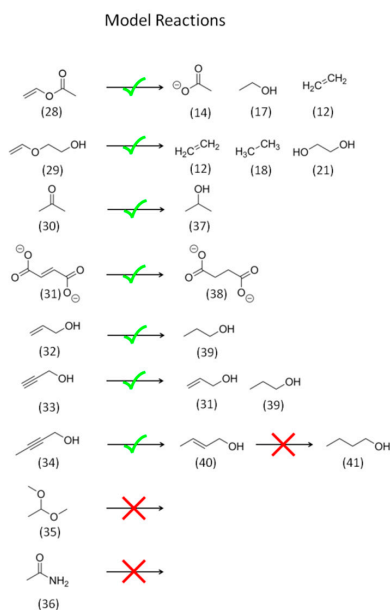
Scheme 2. Model reaction supporting the pathways as depicted in Scheme 1.

2.2.1. Reactivity of CO_2 and HCO_3^-

In order to exclude any perturbation, it was verified that HCO_3^- is inert under these conditions. Electrolysis in an Ar-purged $KHCO_3$ electrolyte indeed yielded only H_2. Importantly, KOH was used as anolyte to ensure that no gaseous CO_2 is liberated at the cation exchange membrane.

2.2.2. Reactivity and Role of $2e^-$ Carboxylate Species

As the screening is related to CO_2 electrolysis, reagents were chosen that derive from CO_2 by 2 electron (e^-) reduction. CO (**2**) is the key intermediate toward all higher reduced products. [20,32,34,35,58]. This could also be verified for the model catalyst. Conclusively, the first key step in our scheme is the reduction of physically dissolved or gaseous CO_2 (**1**) to CO (**2**).

In CO_2 electrolysis, formate (**4**) and oxalate (**5**) as well as their conjugated alcohols methanol (**26**) and ethylene glycol (**21**) are found. Addition of formate (**4**) to the electrolyte under argon purging, however, did not yield any reduction products. Its reduction to methanol is evidently possible as ligand on a heavy metal complex [59], but not on copper cathode with competing HER. Like HCO_3^- (**3**) and CO_2, also formate (**4**) is related to CO (**2**) as its hydrate form. In both cases, only the neutral gaseous form was found to be electrochemically active.

Despite it never having been observed in our system, oxalate (**5**) was also used as reactant. Firstly, it is well known in anhydrous electrolytes, where carboxyl-radicals (**6**) usually dimerise (**6**) → (**5**) instead of being reduced by a hydrogen radical (**6**) → (**4**). Secondly, it is a C2 building block and, therefore, a possible intermediate to ethanol (**17**) or ethylene glycol (**21**). Yet, no evidence for electrochemical conversion of oxalate (**5**) could be found even after passing more than 4 e^- per molecule into the system. Thus, oxalate is a dead end.

2.2.3. Reactivity of Higher Carboxylates

Ethanol (**17**) could arguably also from by reduction of acetate (**14**). However, when adding sodium acetate to our model system, no evidence was found for acetate (**14**) being further reduced to any liquid or gaseous product. This result, together with the results from formate (**4**) and oxalate (**5**), suggests that carboxylates in general are inert to electro-reduction by the in situ-grown copper catalyst. Acetamide (**36**), which in contrast to acetate is not negatively charged, also underwent no transformation. Also carboxylate groups, which are part of an α,β-unsaturated π-system as in fumarate (**31**), remain untouched.

2.2.4. The Role of Acetaldehyde Acyl-Species and Enolates

In the literature, several pathways to hydrocarbon products are discussed. The most widely accepted one begins by formation of a C_2O_2 intermediate and is supported by the work of the Hori [60] and the Koper group [44]. Ma et al., recently proposed a mechanism under high current density conditions, featuring ketene (**13**) and methylene (**10**) as key intermediates [57]. In this mechanism, ethene (**12**) is produced by dimerisation of two methylene (**10**) units. Ethanol (**17**) is formed by carbonylation of one methylene (**10**) to ketene (**13**) and two subsequent reduction steps to acetaldehyde (**16**) and ethanol (**17**). Both these mechanisms feature acetalydehyde (**16**) as an intermediate. In the first mechanism, it is the "Selectivity Determining Intermediate" (SDI) and precursor to ethene (**12**) and ethanol (**17**) [44–46]. In the latter, it is only precursor to ethanol (**17**).

Bertheussen et al. [52] recently reported the observation of considerable quantities of acetaldehyde (**16**) in an authentic electrolysis experiment and demonstrated the authentic bulk electro-hydrogenation of acetaldehyde (**16**). We attempted to reproduce these results and also intended to demonstrate the ethene (**12**) from acetaldehyde (**16**). The affinity of the catalyst towards aldehydes is very high, even under elevated current density conditions. Addition of acetaldehyde (**16**) to a running electrolysis under Ar purging suppressed the HER from 100% to 4%. This affinity was also reflected in the WE

potential, which rose from −1.86 V to −1.39 V vs. Ag/AgCl by addition of the acetaldehyde (**16**) at a current density of 30 mAcm^{-2}.

While we could also confirm the reduction of acetaldehyde (**16**) to ethanol (**17**) under our model conditions, no ethene (**12**) could be found in the gas phase. This contradicts an ethene formation from acetaldehyde (**16**) and rather supports the scheme of Ma et al., where only ethanol (**17**) is formed from acetaldehyde (**16**) [57].

DFT calculation for the C$_2$O$_2$ mechanism suggests that acetaldehyde (**16**) is adsorbed in its enolate form [44–46]. To enforce this tautomeric form, vinyl acetate (**28**) and ethylene glycol vinyl ether (**29**) were used as models for enolates.

Indeed, in both cases ethene (**12**) evolution was observed. Vinyl acetate (**28**) reduction however suffered from the participation of free acetaldehyde (**16**) from saponification of the ester. The bulk of the reagent was actually converted into ethanol (**17**) and acetate (**14**). The appearance of small quantities of *n*-butanol (**41**) proved the presence of free acetaldehyde (**16**). In contrast to the ester, the ether protection group was stable against hydrolysis. Indeed, its addition yielded only ethylene glycol (**21**) in the liquid phase and ethene (**12**) and ethane (**18**) in the gas phase. This can only be explained by an oxidative addition/dissociative adsorption of the vinyl-ether (**29**) into an alcoholate and a copper vinyl complex (**15**), which was then terminated by a hydrogen-radical or reduced. This, on the other hand, supports an ethene (**12**) formation from acetaldehyde (**16**) as featured in the C$_2$O$_2$ based mechanism.

An explanation for these ambiguous results may be different potential and current density regimes. The C$_2$O$_2$ mechanism was derived a specific crystal plane Cu(100) and a potential of −0.4 V−−0.45 V [45,46] vs. RHE.

In the case of this study, a dendritic catalyst was used at around −1.0 V vs. RHE. Under such conditions, other mechanistic pathways on other crystal planes may prevail. This is supported by recent results provided by Surendranath [61] and coworkers, who found a pH-invariant strong rise of the CO-binding ability of copper surface for potentials more negative than −0.6 V and a saturation of CO-binding strength for potentials more negative than −0.8 V. This clearly sets up two different potential regimes. This study and the work of Ma et al. [57] were both executed in a high current density and, therefore, high overpotentials regime. It appears that under high overpotentials, the rate of electro-hydrogenation of acetaldehyde (**16**) vastly exceeds the rate of sp^{2}C–O bond cleavage. However, the reaction can be enforced using protection groups. This again emphasizes that the mechanisms at onset potentials and high current densities are not necessarily comparable.

There appear to be multiple pathways to ethene (**12**), which become accessible under different potentials. Recently, Ledezma-Yanez et al., also reported that the hydrogenation or cleavage of acetaldehyde (**16**) is very site-sensitive [62], which may play an important role on a dendritic catalyst. Nevertheless, the same catalyst that was used for the acetaldehyde reduction yields higher FEs for ethene (**12**) than ethanol (**17**) for CO$_2$RR. The lack of ethene observation therefore cannot be a sole site effect.

The reductive cleavage of vinyl alcohol derivatives is actually a very interesting reaction even if just considered an electrochemical bulk transformation on its own. It is an electrochemical Reverse Wacker Oxidation.

2.2.5. Reactivity of C=O Double Bonds

The mechanistic scheme that is presented here features many electro-hydrogenations of C=O and C=C bonds, which were therefore studied in detail. Aldehydes, as mentioned above, readily undergo electro-hydrogenation to the corresponding alcohols. To further probe the reactivity of C=O double bonds, also acetone (**30**) was evaluated and *i*-propanol (**37**) was obtained. Reactivity-wise, however, already this simplest ketone acetone (**30**) was far less reactive than the aldehydes. The WE potential did not change notably when it was added. Less than 10% were actually converted after passing 4.8 F/mol. It cannot be ruled out that, in case of ketones, the reduction takes place via hydrogen *in statu nascendi*. There are no reliable reports about *i*-propanol (**37**) or any other secondary alcohols in

CO_2RR. In this case, this is due to the low reactivity of the corresponding ketones and, therefore, the lack of an efficient formation pathway.

As origin of acetaldehyde Bertheussen et al. [52] proposed a surface HC_2O_2 intermediate (**22**) towards the formation of acetaldehyde (**16**). Its mono-hydrogenation may yield glyoxal (**20**), which was also found by Kuhl et al. [17]. Subsequent hydrogenation of glyoxal (**20**) yielded ethylene glycol (**21**). In conclusion, glyoxal (**20**) is an intermediate to ethylene glycol (**21**), which is also found in Cu-catalyzed CO_2 reduction, usually at low overpotentials. It should be noted that glyoxal (**20**) also rapidly undergoes benzilic-acid rearrangement [63] when exposed to high pH values as present in the vicinity of the electrode to yield glycolic acid (**23**) [64].

In the C_2O_2-based low overpotential mechanism, the reduction to acetaldehyde (**16**) also proceeds via sp^2C–O bond cleavages. As for acetaldehyde (**16**), also in this case the balance between C–O bond cleavage and C=O bond hydrogenation may shift completely to the latter at higher overpotentials. Ethylene glycol (**21**) evolves at lower overpotentials (>-0.9 V vs. RHE) [17] than those where pronounced ethene (**12**), ethanol (**17**) or acetate (**14**) evolution is observed (<-1.1 V vs. RHE). Thus, C_2O_2 and HC_2O_2 species (**22**) are evidently present at very low overpotentials, as suggested by the Strasser, Chorkendorff and Nørskov groups [16,51,52,65] and may yield acetaldehyde (**16**) as intermediate for ethanol (**17**) and ethene (**12**) evolution at low overpotentials, which yet is no longer valid at high current densities. These conditions, however, are not within the scope of this work.

CO (**2**) and HCO (**7**) species, which are proposed to form C_2O_2 or HC_2O_2 (**22**), are also precursors for methanol (**26**) via formaldehyde (**25**) as intermediate. Formaldehyde (**25**) in the experiment was rapidly reduced and fully converted to methanol (**26**). Noteworthy, no other products were observed. Formaldehyde (**25**) was controversially discussed as intermediate for chain growth in Fischer-Tropsch chemistry [66]. Also for CO_2RR no evidence for C–C bond formation from formaldehyde (**25**) was found. In conclusion, the liberation of formaldehyde (**25**) from surface formyl (**7**) or hydroxycarbene (**8**) species is irreversible.

2.2.6. Reactivity of Alcohols and Ethers

Ethylene glycol (**21**) was also proposed as an intermediate to ethanol (**17**) [17]. The cleavage of ethylene glycol vinyl ether (**28**) has proven that C–O bond cleavage is possible also for non-organometallic intermediates. Addition of ethylene glycol (**21**) to our model electrolysis did not yield any reduction products nor affected potential or HER. Likewise, ethanol (**17**) did not undergo any transformations, for example, to ethane (**18**). In contrast to the aforementioned enol-ether (**29**), acetaldehyde-dimethylacetal (**35**) (Scheme 2) also did not react. It was concluded that, in general, saturated compounds and alcohols are inert towards reduction by an in situ-grown copper electro-catalyst. The C–O single bond cleavage appears to be limited to strongly adsorbed high energy species with multiple bonds to the surface as CO (**2**), hydroxymethylene (**8**), hydroxymethyne [17], and $CO_2\bullet^-$ (**6**), which cannot exist as free molecules in solution or enolates under specific conditions.

The strong driving force for the reduction of such species as opposed to their liberation is reflected in the almost negligible FEs for methanol (**26**) (<0.1%) as opposed to C2 or C3 products with only one oxygen-containing functional group (e.g., ethanol (**17**), acetate (**14**) and *n*-propanol (**39**)) in this system. We have experimentally proven that neither formaldehyde (**25**) nor formate (**4**), once liberated, can be re-adsorbed and reduced to the C1 carbene precursors for ethanol, acetate or ethene (**12**).

2.2.7. Reactivity of Alkenes

The first experiments concerning C=C double bonds were carried out with allyl alcohol (**32**), as both ally alcohol (**32**) and its saturated pendant *n*-propanol (**39**) are present in the CO_2RR product scope. Addition of allyl alcohol (**32**) to the electrolyte while purging with argon yielded *n*-propanol (**39**). Thusly, the formation of *n*-propanol (**39**) proceeds, at least partially, via the intermediate allyl alcohol (**32**), which therefore is never observed in large quantities. The complete discussion of the C3-product scope of copper catalyzed CO_2 reduction is out of scope for this publication. This experiment

authentically demonstrated that electro-hydrogenation of C=C double bonds are feasible reaction steps on the surface of a copper electrode. It is actually quite surprising, that a rather electron-rich alkene like allyl alcohol (**32**), which is therefore deactivated towards reduction, is electro-hydrogenated by the in situ-grown copper catalyst with competing HER.

Some references of copper-catalyzed CO_2RR mention trace amounts of ethane (**18**) [20]. Taking the results with allyl alcohol into concert, we concluded that ethane (**18**) must originate from the in situ electro-hydrogenation of ethene (**12**). This was verified by using ethene (**12**) as feed gas, which was partially reduced to ethane (**18**). The conversion was very low (0.03% conversion, 2.2% FE) and the HER was barely attenuated. This observation is in agreement with literature reports of high ethane (**18**) efficiencies being rare. The ethene (**12**) hydrogenation ability of the in situ-grown copper electro-catalysts and, obviously, most other copper-based systems, is rather poor. Examination of the liquid phase did not show any products, which ruled out that ethanol (**17**) is at least partially produced by in situ hydration of ethene (**12**) → (**17**).

In contrast to ethene (**12**) and allyl alcohol (**32**), electron-poor double bonds are very reactive. This was confirmed by electro-reduction of potassium fumarate (**31**). Potassium succimate (**38**) was observed as sole product of this reaction.

The transformation was particularly interesting as the conversion was quantitative and the HER was completely suppressed after addition. This behavior was also reflected in the WE potential, which dropped from −1.83 V to −1.34 V vs. Ag/AgCl upon addition (also see Figures S9 and S10 in the Supplementary Materials (SM)).

The copper electro-catalyst, in conclusion, has certain ability for alkene hydrogenation yet requires activated substrates. This is in full agreement with the actual CO_2RR product spectrum, which features several electron-rich alkenes, yet no electron-deficient alkenes, and suggests the latter as highly reactive intermediates.

2.2.8. Reactivity of Alkynes

Several even very different mechanistic models incorporate carbyne species [17,44,45]. As the dimerization of carbynes to alkynes is even known to proceed on single metal centers [67], they could also be proposed as intermediates. As models for triple-bond ethyne (**19**), propargyl alcohol (**33**) and 2-butyn-1-ol (**34**) were used. The latter served as model for an internal triple bond. C≡C triple bonds turned out to be surprisingly reactive towards the in situ-grown copper catalyst. In our experiment, the transformation of propargyl alcohol (**33**) to allyl alcohol (**32**) was quantitative with only small amounts of *n*-propanol (**37**) found from further reduction. Allyl alcohol (**32**) as reactant gave much lower conversion of 34% at more charge per moles passed. Also, the addition of propargyl alcohol (**33**) completely suppressed the HER and lowered the WE potential to −1.41 V at 30 mAcm^{-2}, while allyl alcohol was reduced with only 15% FE at −1.67 V.

Reduction of ethyne (**19**) gave ethene (**12**) as major product. Small quantities of ethane (**18**) were also observed. Analysis of the electrolyte showed no further liquid products. The HER could not be totally suppressed probably due to the poor solubility of ethyne (**19**) in water. However, up to 61% of the charge passed went into the reduction of ethyne (**19**) to ethene (**12**) as opposed to 2% ethane (**18**) yield for ethene (**12**) feed. Palladium, a noble metal well known for its hydrogenation activity, was also recently reported to selectively electro-hydrogenate ethyne (**19**) to ethene (**12**) by Song et al. [68]. Finding a similar behavior for copper is a terrific result, not only giving insight to copper-catalyzed CO_2 electro-reduction, but also opening new pathways for organic electro-synthesis.

In all experiments, we found a strong preference for the reduction of triple bonds over double bonds. A straightforward explanation for this may be that terminal alkynes form copper alkynides even in the presence of rather weak bases, which leads to a much stronger adsorption than the π-complexes that are formed by alkenes. In order to clarify the role of alkynides, the internal alkyne 2-butyn-1-ol (**34**) was used as model reactant. The results contradict the alkynide theory. Despite being more sterically hindered and more electronically deactivated, 2-butyn-1-ol (**34**) showed much higher reactivity and

higher conversion than allyl alcohol (**32**). Noteworthy, while the conversion to crotyl alcohol (**40**) was quantitative, *n*-butanol (**41**) was only observed in barely detectable traces, though the charge passed into the system was more than enough (4.8 F/mol passed, 4 needed) to convert the whole sample into *n*-butanol. The resulting crotyl alcohol (**40**) is already too sterically hindered to be reduced by the copper catalyst in aqueous environment. The effect on the WE potential for 2-butyn-1-ol (**34**) was not as pronounced as for terminal alkenes and more comparable to allyl alcohol (**32**). The participation of acetylide species (**9**) in the case of terminal alkenes therefore cannot be fully ruled out. Yet, it is not the sole explanation for the high reactivity of triple bonds toward Cu-catalyzed electro-reduction.

As for electron-deficient alkenes, also in the case of alkynes, their high reactivity rather renders them highly reactive intermediates than products without formation pathway. Due to these results, we propose the participation of ethyne (**19**) and vinyl (**15**) species in the formation of ethene (**12**). The first can be formed from carbyne–carbyne (**9,9**) coupling on the surface, the latter from carbyne–carbene (**9,10**) coupling or re-adsorption and one electron reduction of ethyne (**19**). We found a high reduction activity of in situ-grown copper electro-catalysts toward C≡C triple bonds. It appears plausible that ethyne (**19**) may be formed as intermediate but is quantitatively reduced to ethene (**12**) and therefore not observed.

It is worth mentioning that carbene (**10**) and carbyne (**9**) species are also featured in the C_2O_2 mechanism as intermediates towards methane (**27**) but not ethene (**12**) [44–46]. At very small conversion rates, the population of methylene units may indeed be too low for a reasonable rate of dimerisation. At elevated current densities and the corresponding high overpotentials and conversion rates, dimerisation becomes more feasible and may prevail over ethene (**12**) formation from acetaldehyde (**16**) which in this regime is exclusively reduced to ethanol (**17**). The same concept also applies to carbyne (**9**) intermediates, which can either dimerise to the evidently rapidly reduced ethyne (**19**) or be coupled with methylene (**10**) to vinyl (**15**) species that also yield ethene (**12**).

2.3. CO Bulk Electrolysis at High Current Density

From the perspective of CO_2 reduction, the most straightforward model reactant is actually CO (**2**). Thusly, we chose to directly compare CO_2 (**1**) and CO (**2**) under identical high current density conditions (Figure 2). Like in the original publication [54], these experiments were conducted with gas diffusion electrodes at 170 mAcm^{-2}.

In analogy to the CO_2 benchmark, the gaseous and liquid products were sampled every 10 min. CO (**2**) electrolysis yielded a product distribution, that was surprisingly similar to the one observed with CO_2 (**1**) under the same conditions.

Thus, CO (**2**) is key intermediated to most products, which also corresponds to current literature [50,52,58,61]. The most prominent difference was the absence of formate (**4**) as product. As we have shown, this electro-catalyst is not capable of formate reduction. Thus, formate (**4**) is exclusively formed from CO_2 (**1**).

As for CO_2 reduction, the catalyst also showed a good selectivity for carbon products, but with a different product distribution pattern.

The FE of acetate (**14**) (yellow in Figure 2) reached 11% after 40 min, which corresponds to 18.7 mAcm^{-2} specific current density. Compared to the CO_2 bulk electrolysis, this is an increase of 300% in the total amount formed and a factor of two in FE. The effect was less pronounced for ethanol (**17**). The FE was increased to 29% (light green in Figure 2) and the specific current density reached 49.8 mAcm^{-2}. Nevertheless, this still results in a 90% increase of ethanol (**17**) formation rate and is the highest ever reported specific current density for ethanol formation from CO (**2**).
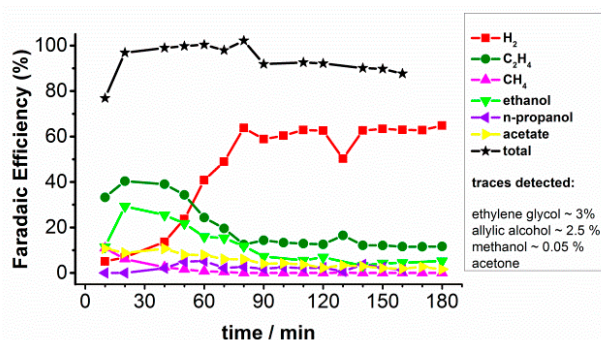
Figure 2. FE vs. time for major products of CO bulk electrolysis at 170 mAcm^{-2}.

Mechanistic Conclusions: Acetate and Ketene

The massive increase of acetate (**14**) formation in the case of CO (**2**) feed may lead to several mechanistic conclusions. It demonstrates that the acetate (**14**) does not originate from nucleophilic reactions between surface methyl species (**11**) and CO_2 (**1**) as its formation is even enhanced in absence of CO_2 (**1**). In fact, the formation of acetate is not covered by the C_2O_2 mechanism [44–46]. This is different for the scheme suggested by Ma et al., The formation of ketene (**13**) from CO (**2**) and methylene (**10**) is a well-known reaction in molecular organometallic chemistry of copper, nickel and iron [69–71]. Several publications also show that the dimerisation of methylene (**10**) and the carbonylation to ketene (**13**) are competing reactions and the carbonylation can proceed by coupling with endogenous and capture of exogenous CO (**2**) [72,73]. Introducing an additional path to Ma's scheme, where ketene is not reduced to acetaldehyde (**16**) but hydrated, explains the occurrence of acetate (**14**) in straightforward manner in line with known chemical reactivity.

In the comparison experiment, both putative products of ketene (**13**), ethanol (**17**) and acetate (**14**), were significantly pronounced, while ethene (**12**) showed the same current yield. This goes well with the model of ketene (**13**) as "Selectivity Determining Intermediate" (SDI) for ethanol (**17**) and acetate (14), as its formation is promoted by a higher abundance of CO (**2**). Ethene (**12**) formation, on the other hand, is not affected by the CO (2) concentration. As methylene (10) dimerisation does not involve CO (**2**) addition, this points to methylene (**10**) as "SDI" for ethene (**12**) and ethanol (**17**)/acetate (**14**). Surendranth and coworkers have recently proven that under high current densities, CO_{ads} is in a potential-invariant quasi equilibrium with CO_{free} [61]. This would also support an enhancement for carbonylation reaction in presence of high CO concentrations.

3. Materials and Methods

Electrolytes were prepared form deionised water (ISO 3686) with a resistance of 18.2 MΩcm^{-1} (Milli-Q Advantage A10 water purification system: Merck, Darmstadt, Germany). KBr and KOH were purchased from Alpha Aesar (Haverhill, MA, USA) in >99% and p.a. purity. 5N $CuSO_4$ purchased from Alpha Aesar (Haverhill, MA, USA) and recrystallised once from water prior to use.

4.5N CO_2, 4.7N CO, 4.5N ethylene, 4.5N methane and solvent free ethyne were purchased from Linde AG (Munich, Germany). The examined model compounds were purchased from ABCR (Karlsruhe, Germany) and Sigma Aldrich (St. Louis, MO, USA) in p.a. or better quality and used without further purification. 5N H_2SO_4 was purchased from Alpha Aesar (Haverhill, MA, USA) and used as received.

Deuterated solvents and internal NMR standards were purchased form Sigma Aldrich (St. Louis, MO, USA).

Carbon GDL's were purchased from FuelCellsEtc (College Station, TX, USA). Electrochemical measurements were conducted on a Metrohm Autolab PGSTAT302N potentiostate-galvanostate (Deutsche Methrom GmbH & Co KG, Filderstadt, Germany).

Gas composition was analyzed on a Thermo Scientific Trace 1310 gas chromatograph (Thermo Fisher Scientific, Waltham, MA, USA) (custom setup purchased from S+H Analytik, Mönchengladbach, Germany). Carbon monoxide, ethylene, ethane, methane and carbon dioxide were separated on a Shincarbon™ column (Restek, Bellefonte, PA, USA) using He as carrier coupled to a thermal conductivity detector (TCD). Hydrogen was analyzed on a 5 Å molecular sieves column (Restek, Bellefonte, PA, USA) with Ar carrier also coupled to a TCD.

NMR Spectra were recorded on a Bruker Avance 400 (400 MHz) NMR spectrometer (Bruker, Billerica, MA, USA) equipped with a Autotune BBO, 5 mm, ^{109}Ag-^{31}P probehead and pulsed field gradient unit. NMR spectra were recorded using the "composite pulses"—presaturation pulse sequence for water suppression. For each spectrum 32 scans were accumulated. The D1-delay was set to 4 s to ensure total spin relaxation after each pulse. NMR-samples were prepared according to the following protocol. To 300 μL of electrolyte 250 μL of D_2O and 50 μL of an internal standard stock solution was added. A 1.2 M aqueous solution of dimethylsulfone ($DMSO_2$) was used as internal standard. For experiments with CO feed a 0.06 M solution of potassium fumarate was used as we found that $DMSO_2$ is prone to undergo H/D-exchange with the solvent under elevated pH-values as present in our CO-feed experiments.

Experiments with CO_2, CO, potassium formate and sodium acetate were conducted in a stacked flow cell purchased from ElectroCell (Tarm, Denmark) (see Figure S1 (SM) for exact configuration). Anolyte and catholyte are pumped through the cell in 2 separate cycles by a peristaltic pump (Ismatec, Wertheim, Germany) at 100 mL/min. Hydrophobic carbon based commercial gas diffusion layers of the types Freudenberg H2315 C2™ and Sigracet 25 BC™ were used as working electrode blanks. The GDLs show comparable results. Figures 1 and 2 show result received on the Freundenberg GDL. The GDL was mounted in a Capton®-sealed Cu-ETP frame with an electrochemically active area of 3.3 cm^2. CO_2/CO was supplied from behind and flowed through the GDL and the in situ grown copper layer into the electrolyte. The gases were fed with 50 sccm against atmospheric pressure using Bronkhorst (Ruurlo, The Netherlands) el-flow™ mass flow controllers. An Ag/AgCl/3M KCl electrode (ALS, Tokyo, Japan) was used as reference electrode. An IrO$_x$ coated Ti-sheet, which was purchased from ElectroCell (Tarm, Denmark) served as counter electrode with an active area of 10 cm^2 active area. The electrolyte compartments were separated by a Nafion N 117 (DuPont, Wilmington, DE, USA) membrane to prevent crossover of products and reagents. The pH-value in the electrolyte reservoir was recorded using a Methrom Unitrode™ (Deutsche Methrom GmbH Co KG, Filderstadt, Germany) coupled to a pX-1000 module™ in the workstation. The overall voltage was monitored on a second pX-1000 module™ (Deutsche Methrom GmbH & Co KG, Filderstadt, Germany).

An aqueous solution of 0.1 M KBr was used as cathoyte and 2.5 M KOH as anolyte. 6.5 mM $CuSO_4$ was added to the catholyte as copper source for in situ catalyst preparation. The initial pH-value of the electrolyte was adjusted to 2 by addition of 0.005 M sulfuric acid.

Bulk electrolysis was conducted in galvanostatic mode at 170 mAcm^{-2} for 3 h. During this time the gas stream was sampled in gas tight bags over 10 min intervals. In parallel 1 mL aliquots of the catholyte were sampled every 10 min.

Reactivity experiments were conducted in an H-type glass cell (custom cell, manufactured by Normag Labor- und Prozesstechnik GmbH, Ilmenau, Germany) with 5 mL electrolyte volume (per electrode), a 1 cm^2 polished Cu sheet working electrode, Ag/AgCl 3M KCl reference electrode (ALS, Tokyo, Japan) and Pt-wire counter electrode. Nafion N117 was used as separator. Electrolytes had the same composition as in the flow cell setup. The reactivity essay was conducted after the following procedure. The catalyst was grown over a period of 10 min at a total current of 30 mA and continuous 10 sccm Ar purging. After this period the model reactant was added. Gases were supplied with 10 sccm. Solids were weighed to 0.5 mM and added dissolved in a small amount of electrolyte. Liquids were added neat in and 32 or 50 μL aliquot. Solid acids were neutralized with an equimolar amount of 5 M KOH prior to addition.

4. Conclusions

The cathodic reactivity of the previously presented in situ-grown copper catalyst towards various small molecules and functional groups was studied in detail. The spectrum of gaseous and liquid products of every transformation was fully characterized.

Several transformations, which were suggested by literature or DFT predictions such as the formation from ally alcohol to *n*-propanol, acetaldehyde to ethanol, ethane to ethane or glyoxal to ethylene glycol, were demonstrated.

The reductive cleavage of enols, which is a central reaction in the low overpotential evolution of ethene from acetaldehyde as intermediate, could be experimentally verified by the cleavage of two vinyl alcohol derivatives. However, the high current density formation of ethene from free acetaldehyde itself was not possible on the investigated catalyst. Reduction to ethanol is highly preferred in this system. Therefore, its high yield of ethene in CO_2 and CO reduction must be formed on another pathway. An ethene formation by methylene dimerisation as suggested by Ma et al., was found feasible and the scheme could be even extended for further products, such as acetate, methanol or ethylene glycol.

The reduction of carboxylates was excluded for five model reagents.

The appearance of alkene products such as ethene and allyl alcohol was found to originate from a poor electro-hydrogenation capability of the copper catalyst.

The absence of secondary alcohols, aldehydes, electron-deficient alkenes and alkynes was elucidated with different results. Secondary alcohols cannot be formed due to the low ketone reduction activity of the catalyst. Aldehydes, electron-deficient alkenes and alkynes, on the other hand, are surprisingly efficiently hydrogenated by the in situ-grown copper catalyst yielding functional groups present in the CO_2RR product scope. Putative intermediates such as ethyne, ketene or acrolein therefore cannot be observed in the electrolyte or with high surface concentrations, especially at the high overpotentials at which they are proposed. Further studies are required to clarify their presence.

References

1. DENA Grid Study II. Available online: http://www.dena.de/fileadmin/user_upload/Projekte/Erneuerbare/Dokumente/dena_Grid_Study_II_-_final_report.pdf (accessed on 17 March 2016).
2. DENA Verteilernetzstudie. Available online: http://www.dena.de/fileadmin/user_upload/Projekte/Energiesysteme/Dokumente/denaVNS_Abschlussbericht.pdf (accessed on 17 March 2016).
3. Sridhar, N.; Agarwal, A.; Rode, E. *Electrochemical Production of Chemicals—Applicability of CO_2 Conversion*; Det Norse Veritas AS: Oslo, Norway, 2012.
4. Schlögl, R. The Role of Chemistry in the Energy Challenge. *ChemSusChem* **2010**, *3*, 209–222. [CrossRef] [PubMed]
5. Qiao, J.; Liu, Y.; Hong, F.; Zang, J. A review of catalysts for the electroreduction of carbon dioxide to produce low-carbon fuels. *Chem. Soc. Rev.* **2014**, *43*, 631–675. [CrossRef] [PubMed]
6. Hori, Y. *Modern Aspects of Electrochemistry*; Vayenas, C.G., White, R.E., Eds.; Springer: New York, NY, USA, 2008; p. 16. ISSN: 0076-9924.

7. Hori, Y. *Handbook of Fuel Cells—Fundamentals, Technology and Applications*; Vielstich, W., Lamm, A., Gasteiger, H.A., Eds.; Wiley VCH: Weinheim, Germany, 2003; ISBN 047-1-49-9269.

8. Paik, W.; Andersen, T.N.; Eyring, H. Kinetic studies of the electrolytic reduction of carbon dioxide on the mercury electrode. *Electrochim. Acta* **1969**, *14*, 1217–1232. [CrossRef]

9. Hori, Y.; Suzuki, S. Electrolytic Reduction of Carbon Dioxide at Mercury Electrode in Aqueous Solution. *Bull. Chem. Soc. Jpn.* **1982**, *55*, 660–665. [CrossRef]

10. Hori, Y.; Kikuchi, K.; Shin Suzuki, K. Production of CO and CH_4 in electrochemical reduction of CO_2 at Metal Electrodes in aqueous hydrogencarbonate solution. *Chem. Lett.* **1985**, *14*, 1695–1698. [CrossRef]

11. Cook, R.L.; MacDuff, R.C.; Sammels, A.F. On the Electrochemical Reduction of Carbon Dioxide at In Situ electrodeposited Copper. *J. Electrochem. Soc.* **1988**, *135*, 1320–1326. [CrossRef]

12. Cook, R.L.; MacDuff, R.C.; Sammels, A.F. High Rate Gas Phase CO_2 Reduction to Ethylene and Methane using Gas Diffusion Electrodes. *J. Electrochem. Soc.* **1990**, *137*, 607–608. [CrossRef]

13. Hori, Y.; Murata, A.; Takahashi, R. Formation of hydrocarbons in the electrochemical reduction of carbon dioxide at copper electrodes in aqueous solution. *J. Chem. Soc. Faraday Trans.* **1989**, *85*, 2309–2326. [CrossRef]

14. Jermann, B.; Augustynski, J. Long-term activation of the copper cathode in the course of CO_2 reduction. *Electrochim. Acta* **1994**, *39*, 1891–1896. [CrossRef]

15. Ogura, K.; Yano, H.; Shirai, F. Catalytic Reduction of CO_2 to Ethylene by Electrolysis at a Three-Phase Interface. *J. Electrochem. Soc.* **2003**, *150*, D163–D168. [CrossRef]

16. Verela, A.S.; Kroschel, M.; Reier, P.; Strasser, P. Controlling the selectivity of CO_2 electroreduction on copper: The effect of the electrolyte concentration and the importance of the local pH. *Catal. Today* **2016**, *260*, 8–13. [CrossRef]

17. Kuhl, K.P.; Cave, E.R.; Abram, D.N.; Jaramillo, T.F. New insights into the electrochemical reduction of carbon dioxide on metallic copper surfaces. *Energy Environ. Sci.* **2012**, *5*, 7050–7059. [CrossRef]

18. Li, C.W.; Kanan, M.W. CO_2 Reduction at Low Overpotential on Cu Electrodes Resulting from the reduction of Thick Cu_2O Films. *J. Am. Chem. Soc.* **2012**, *134*, 7231–7234. [CrossRef] [PubMed]

19. Chi, D.; Yang, H.; Du, Y.; Lu, T.; Sui, G.; Wang, H.; Lu, J. Morphology-controlled CuO nanoparticles for the electroreduction of CO_2 to ethanol. *RCS Adv.* **2014**, *4*, 37329–37332.

20. Kas, R.; Kortlever, R.; Milbrat, A.; Koper, M.T.M.; Maul, G.; Baltrisaitis, J. Electrochemical CO_2 reduction on Cu_2O-derived copper nanoparticles: Controlling the selectivity of hydrocarbons. *Phys. Chem. Chem. Phys.* **2014**, *16*, 12194–12201. [CrossRef] [PubMed]

21. Mistry, H.; Varela, A.S.; Bonifacio, C.S.; Zegkinoglou, I.; Sinev, I.; Choi, Y.-W.; Kisslinger, K.; Stach, E.A.; Yang, J.C.; Strasser, P.; et al. Highly selective plasma-activated copper catalysts for carbon dioxide reduction to ethylene. *Nat. Commun.* **2016**, *7*, 12123. [CrossRef] [PubMed]

22. Schwartz, M.; Cook, R.L.; Kehoe, V.M.; MacDuff, R.C.; Patel, J.; Sammells, A.F. Carbon Dioxide Reduction to Alcohols using Perovskite-Type Electrocatalysts. *J. Electrochem. Soc.* **1993**, *140*, 614–618. [CrossRef]

23. Jermann, B. *Réduction Electrochimique de Longue Durée du Dioxyde de Carbone sur des Cathodes en Cuivre*; Université de Genéve: Geneva, Switzerland, 1995.

24. Chen, C.S.; Handoko, A.D.; Wan, J.H.; Ma, L.; Ren, D.; Yeo, B.S. Stable and selective electrochemical reduction of carbon dioxide to ethylene on copper mesocrystals. *Catal. Sci. Technol.* **2015**, *5*, 161–168. [CrossRef]

25. Yano, H.; Tanaka, T.; Nakayama, M.; Ogura, K. Selective electrochemical reduction of CO_2 to ethylene at a three-phase interface on copper(I) halide-confined Cu-mesh electrodes in acidic solutions of potassium halides. *J. Electroanal Chem.* **2004**, *565*, 287–293. [CrossRef]

26. Ogura, K.; Oohara, R.; Kudo, Y. Reduction of CO_2 to Ethylene at Three-Phase Interface Effects of Electrode Substrate and Catalytic Coating. *J. Electrochem. Soc.* **2005**, *152*, D213–D219. [CrossRef]

27. Albo, J.; Sáez, A.; Solla-Gullón, J.; Montiel, V.; Irabien, A. Production of methanol from CO_2 electroreduction at Cu_2O and Cu_2O/ZnO-based electrodes in aqueous solution. *Appl. Catal. Environ.* **2015**, *176*, 709–717. [CrossRef]

28. Grote, J.-P.; Zeradjanin, A.R.; Cherevko, S.; Savan, A.; Breitbach, B.; Ludwig, A.; Mayrhofer, K.J.J. Screening of material libraries of electrochemical CO2 reduction catalysts—Improving the selectivity of Cu by mixing with Co. *J. Catal.* **2016**, *343*, 248–256. [CrossRef]

29. Albo, J.; Vallejo, D.; Beobide, G.; Catillo, O.; Irabien, A. Copper-Based Metal-Organic Porous Materials for CO_2 Electrocatalytic Reduction to Alcohols. *ChemSusChem* **2017**, *6*, 1100–1109. [CrossRef] [PubMed]

30. Huan, T.N.; Andreiadis, E.S.; Heidkamp, J.; Simon, P.M.; Derat, E.; Cobo, S.; Royal, G.; Bergmann, A.; Strasser, P.; Dau, H.; et al. From molecular copper complexes to composite electrocatalytic materials for selective reduction of CO_2 to formic acid. *J. Mater. Chem. A* **2015**, *3*, 3901–3907. [CrossRef]

31. Gatrell, M.; Gupta, N.; Co, A. A review of the aqueous electrochemical reduction of CO_2 to hydrocarbons on copper. *J. Electroanal. Chem.* **2006**, *594*, 1–19. [CrossRef]

32. Jitaru, M. Electrochemical Carbon Dioxide Reduction—Fundamental and Applied Topics. *J. Univ. Chem. Technol. Metall.* **2007**, *42*, 333–344.

33. Oloman, C.; Lui, H. Electrochemical Processing of Carbon Dioxide. *ChemSusChem* **2008**, *1*, 385–391. [CrossRef] [PubMed]

34. Mikkelsen, M.; Jørgensen, M.; Krebs, F.C. The teraton challenge. A review of fixation and transformation of carbon dioxide. *Energy Environ. Sci.* **2010**, *3*, 43–81. [CrossRef]

35. Whipple, D.T.; Kenis, P.J.A. Prospects of CO_2 Utilization via Direct Heterogeneous Electrochemical Reduction. *J. Phys. Chem. Lett.* **2010**, *1*, 3451–3458. [CrossRef]

36. Neubauer, S.S.; Krause, R.K.; Schmid, B.; Guldi, D.M.; Schmid, G. Overpotentials and Faraday Efficiencies in CO_2 Electrocatalysis—The Impact of 1-Ethyl-3-Methylimidazolium Trifluormethanesulfonate. *Adv. Energy Mater.* **2016**, *6*, 1502231. [CrossRef]

37. Seshadri, G.; Lin, C.; Bocarsly, A.B. A new homogeneous electrocatalyst for the reduction of carbon dioxide. *J. Electroanal. Chem.* **1994**, *372*, 145–150. [CrossRef]

38. Albo, J.; Beobide, G.; Castano, P.; Irabien, A. Methanol Synthesis from CO_2 at Cu_2O/ZnO promoted by pyridine-based aqueous solutions. *J. CO2 Util.* **2017**, *18*, 164–172. [CrossRef]

39. Torelli, D.A.; Francis, S.A.; Crompton, J.C.; Javiert, A.; Thompson, J.R.; Brunschwig, B.S.; Soriaga, M.P.; Lewis, N.S. Nickel-Gallium-Catalyzed Electrochemical Reduction of CO_2 to Highly Reduced Products at Low Overpotentials. *ACS Catal.* **2016**, *6*, 2100–2104. [CrossRef]

40. Shen, J.; Kortlever, R.; Kas, R.; Birdja, Y.Y.; Diaz-Morales, O.; Kwon, Y.; Ledezma-Yanez, I.; Schouten, K.J.P.; Mul, G.; Koper, M.T.M. Electrocatalytic reduction of carbon dioxide to carbon monoxide and methane at an immobilized cobalt protoprophyrin. *Nat. Commun.* **2016**, *6*, 8177. [CrossRef] [PubMed]

41. Peterson, A.A.; Abild-Pedersen, F.; Studt, F.; Rossmeisl, J.; Nørskov, J.K. How copper catalyzes the electroreduction of carbon dioxide into hydrocarbon fuels. *Energy Environ. Sci.* **2010**, *3*, 1311–1315. [CrossRef]

42. Nørskov, J.K.; Abild-Pedersen, F.; Studt, F.; Bligaard, T. Density functional theory in surface chemistry and catalysis. *Proc. Natl. Acad. Sci. USA* **2011**, *108*, 937–943. [CrossRef] [PubMed]

43. Durand, W.J.; Peterson, A.A.; Peterson, F.; Studt, F.; Abild-Pedersen, F.; Nørskov, J.K. Structure effects on the energetics of the electrochemical reduction of CO_2 by copper surfaces. *Surf. Sci.* **2011**, *605*, 1254–1359. [CrossRef]

44. Schouten, K.J.P.; Kwon, Y.; van der Ham, C.J.M.; Qim, Z.; Koper, M.T.M. An new mechanism for the selectivity to C_1 and C_2 species in the electrochemical reduction of carbon dioxide on copper electrodes. *Chem. Sci.* **2011**, *2*, 1902–1909. [CrossRef]

45. Kortlever, R.; Shen, J.; Schouten, K.J.P.; Calle-Vallejo, F.; Koper, M.T.M. Catalysts and Reaction Pathways for the Electrochemical Reduction of Carbon Dioxide. *J. Phys. Chem. Lett.* **2015**, *6*, 4073–4082. [CrossRef] [PubMed]

46. Calle-Vallejo, F.; Koper, M.T.M. Theoretical Conciderations on the Electroreduction of CO to C_2 Species on Cu(100) Electrodes. *Angew. Chem. Int. Ed.* **2013**, *52*, 7282–7285. [CrossRef] [PubMed]

47. Nie, X.; Esopi, M.R.; Janik, M.J.; Asthagiri, A. Selectivity of CO_2 Reduction on Copper Electrodes: The Role of the Kinetics of Elemententary Steps. *Angew. Chem. Int. Ed.* **2013**, *52*, 2459–2462. [CrossRef] [PubMed]

48. Ren, D.; Deng, Y.; Handoko, A.D.; Chem, C.S.; Malkhandi, S.; Yeo, B.S. Selective Electrochemical Reduction of Carbon Dioxide to Ethylene and Ethanol of Copper(I)Oxide Catalysts. *ACS Catal.* **2015**, *5*, 2814–2821. [CrossRef]

49. Kim, D.; Lee, S.; Ocon, J.D.; Jeong, B.; Lee, J.K.; Lee, J. Insights into an autonomously formed oxygen-evacuated Cu_2O electrode for the selective production of C_2H_4 from CO_2. *Phys. Chem. Chem. Phys.* **2015**, *17*, 824–830. [CrossRef] [PubMed]

50. Schouten, K.J.P.; Qin, Z.; Gallent, E.P.; Koper, M.T.M. Two Pathways for the formation of Ethylene in CO Reduction on Single-Crystal Copper Electrodes. *J. Am. Chem. Soc.* **2012**, *134*, 9864–9867. [CrossRef] [PubMed]

51. Tang, W.; Peterson, A.A.; Varela, A.S.; Jovanov, Z.P.; Bech, L.; Durand, W.J.; Dahl, S.; Nørskov, J.K.; Chrokendorff, I. The importance of surface morphology in contolling the selectivity of polycrystalline copper for CO_2 electroreduction. *Phys. Chem. Chem. Phys.* **2012**, *14*, 76–81. [CrossRef] [PubMed]

52. Bertheussen, E.; Verdaguer-Casadevall, A.; Ravasio, D.; Montoya, J.H.; Trimarco, D.B.; Roy, C.; Meier, S.; Wendland, J.; Nørskov, J.K.; Stephens, I.E.L.; et al. Acetaldehyde as an intermediate in the Electroreduction of Carbon Monoxide to Ethanol on Oxide-Derived Copper. *Angew. Chem. Int. Ed.* **2016**, *55*, 1450–1454. [CrossRef] [PubMed]

53. Reller, C.; Krause, R.K.; Neubauer, S.S.; Schmid, G.; Fleischer, M. CO_2-to-value direct electrocatalytic reduction of CO_2 towards chemical feedstock. In Proceedings of the 48 Jahrestreffen Deutscher Katalytiker, Congress Centrum Neue Weimarhalle, Weimar, Germany, 11–13 March 2015.

54. Reller, C.; Krause, R.; Volkova, E.; Schmid, B.; Neubauer, S.; Rucki, A.; Schuster, M.; Schmid, G. Selective Electroreduction of CO_2 toward Ethylene on Nano Dendritic Copper Catalysts at High Current Density. *Adv. Energy Mater.* **2017**. [CrossRef]

55. Kim, Y.-G.; Javier, A.; Baricuatro, J.H.; Soriaga, M.P. Regulating the Product Distribution of CO Reduction by the Atomic Level Structural Modification of the Cu Electrode Surface. *Electrocatalysis* **2016**, *7*, 391–399. [CrossRef]

56. Zinola, C.F. *Electrocatalyis: Computational, Experimental and Industrial Aspects*; CRC Press: Boca Raton, FL, USA, 2010; ISBN 978142004544.

57. Ma, S.; Sadakiyo, M.; Luo, R.; Heima, M.; Yamauchi, M.; Kenis, P.J.A. One-step electrosynthesis of ethylene and ethanol from CO_2 in an alkaline electrolyzer. *J. Power Sources* **2016**, *301*, 219–228. [CrossRef]

58. Li, C.W.; Ciston, J.; Kanan, M.W. Electroreduction of Carbon Monoxide to Liquid Fuels on Oxide-Derived Nanocrystalline Copper. *Nature* **2014**, *508*, 504–520. [CrossRef] [PubMed]

59. Wesselbaum, S.; Moha, V.; Meuresch, M.; Brosinski, S.; Thenert, K.M.; vom Stein, T.; Englert, U.; Hölscher, M.; Klankermeyer, J.; Leitner, W. Hydrogenation of carbon dioxide to methanol using a homogeneous ruthenium-Triphos catalyst: From mechanistic investigations to multiphase catalysis. *Chem. Sci.* **2015**, *6*, 693–704. [CrossRef]

60. Murata, Y.; Hori, Y. Product Selectivity Affected by Cationic Species in Electrochemical Reduction of CO_2 and CO at a Cu Electrode. *Bull. Chem. Soc. Jpn.* **1991**, *64*, 123–127. [CrossRef]

61. Wuttig, A.; Liu, C.; Peng, Q.; Yaguchi, M.; Hendon, C.H.; Motobayashi, K.; Ye, S.; Osawa, M.; Surendranath, Y. Tracking a Common Surface-Bound Intermediate during CO_2-to-Fuels Catalysis. *ACS Cent. Sci.* **2016**, *2*, 522–528. [CrossRef] [PubMed]

62. Ledezma-Yanes, I.; Pérez Gallent, E.; Koper, M.T.M.; Calle-Vallejo, F. Structure-sensitive electroreduction of acetaldehyde to ethanol on copper and its mechanistic implications for CO and CO_2 reduction. *Catal. Today* **2016**, *262*, 90–94. [CrossRef]

63. Loeffler, K.W.; Koehler, C.A.; Paul, N.M.; De Haan, D.O. Oligomer formation in evaporating aqueous glyoxal and methyl glyocal solutions. *Environ. Sci. Technol.* **2006**, *40*, 6318–6323. [CrossRef] [PubMed]

64. Gupta, N.; Gattrell, M.; MacDougall, B. Calculations for the cathode surface concentrations in the electrochemical reduction of CO_2 in $KHCO_3$ solutions. *J. Appl. Electrochem.* **2006**, *36*, 161–172. [CrossRef]

65. Montoya, J.H.; Peterson, A.A.; Nørskov, J.K. Insights into C–C coupling in CO_2 Electroreduction on Copper Electrodes. *ChemCatChem* **2013**, *5*, 737–742. [CrossRef]

66. Kropp, K.; Skibbe, V.; Erker, G.; Krueger, C. Fischer-Tropsch intermediates: Tris[(.eta.2-formaldehyde) zirconocene] from the carbonylation of a zirconium hydride. *J. Am. Chem. Soc.* **1983**, *105*, 3353–3354. [CrossRef]

67. Suess, D.L.M.; Peters, J.C. A CO-Derived Iron Dicarbyne That Releases Olefin upon Hydrogenation. *J. Am. Chem. Soc.* **2013**, *135*, 12580–12583. [CrossRef] [PubMed]

68. Song, X.; Du, H.; Liang, Z.; Zhu, Z.; Duan, D.; Liu, S. Paired Electrochemical Synthesis of Ethylene and Oxalic Acid from Acetylene. *Int. J. Electrochem. Sci.* **2013**, *8*, 6566–6573.

69. Rüchardt, C.; Schrauzer, G.N. Über die Carbonylierung von Carbenen und die katalytische Zersetzung von Diazoalkanen mit Nickeltetracarbonyl. *Chem. Ber.* **1960**, *93*, 1840–1848. [CrossRef]

70. Mankad, N.P.; Peters, J.C. Diazoalkanes react with a bis(phosphino)borate copper(I) source to generate $[Ph_2BP^{tbu}_2]Cu(\eta^1$-$N_2CR_2),[Ph_2BP^{tBu}_2]Cu(CPh_2)$, and $[Ph_2BP^{tbu}_2]Cu$-$N(CPh_2)(NCPh_2)$. *Chem. Commun.* **2008**, 1061–1063. [CrossRef] [PubMed]

71. Dai, X.; Warren, T.H. Discrete Bridging and Terminal Copper Carbenes in Copper-Catalyzed Cyclopropanation. *J. Am. Chem. Soc.* **2004**, *126*, 10085–10094. [CrossRef] [PubMed]

72. Grotjahn, D.B.; Bikzhanova, G.B.; Collins, L.S.B.; Concolino, T.; Lam, K.-C.; Rheingold, A.L. Controlled, Reversible Conversion of a Ketene Ligand to Carbene and CO Ligands on a Single Metal Center. *J. Am. Chem. Soc.* **2000**, *122*, 5222–5223. [CrossRef]

73. Bodnar, T.W.; Cutler, A.R. Formation of a stable (.eta.2-C,C) ketene compound dicarbonyl(cyclopentadienyl) keteneiron hexafluorophosphate [$(C_5H_5)Fe(CO)_2(CH2CO)^+$ PF_6^-] by carbonylation of an iron methylidene complex. A novel entry into carbonyl-derived C2 chemistry. *J. Am. Chem. Soc.* **1983**, *105*, 5926–5928. [CrossRef]